Modeling Polarization through Induced Atomic Charges

György G. Ferenczy*,† and Christopher A. Reynolds‡

Department of Inorganic Chemistry and Department of Chemical Information Technology, Budapest University of Technology and Economics, Szent Gellért tér 4, H-1111 Budapest, Hungary, and Department of Biological Sciences, University of Essex, Wivenhoe Park, Colchester, Essex CO4 3SQ, United Kingdom

Received: May 10, 2001; In Final Form: September 25, 2001

A distributed atomic charge model to account for intermolecular polarization is presented. The model is an approximation to the method of calculating induced dipoles from atomic polarizabilities. In this model, induced atomic dipoles are represented by charges on the atom itself plus neighboring atomic sites. The model therefore avoids the evaluation of charge−dipole and dipole−dipole interactions. Formulas for calculating the induced atomic charges are presented and the approximations involved are discussed. Numerical examples show that our model recovers a substantial part of the polarization energy while the gain in computational efficiency with respect to the induced dipole model is 2−4-fold, being in the upper range when gradients are also evaluated. The use of moments induced by permanent charges only, i.e., calculated without iteration, was found to give an effective approximation with a gain in computational efficiency of up to 7-fold. Analysis of the numerical discrepancies between the induced charge and the induced dipole model showed that the induced atomic charge model of polarization has a 10−40% error for close molecular interactions with the error at the lower end for water−water interactions at equilibrium geometries and it gives an improving approximation with increasing intermolecular separations. The ability of the induced charge model to improve the nonpolarizable TIP3P water model was investigated by comparing the properties of liquid water (e.g., density, diffusion coefficient, radial distribution function) predicted by molecular dynamics simulations. A noniterative polarization model combined with parameters consistent with experimental data (geometry, vacuum dipole moment, polarizability) and with adjusted Lennard-Jones parameters was shown to give properties in good agreement with experimental data. This result suggests that an effective polarizable force field can be built by combining the induced charge model with further energy components. It is argued that the induced charge model represents a significant step toward the best available distributed charge approximation to the induced dipole model and so conclusions drawn for the performance of the model bear significance to other distributed charge models.

1. Introduction

Classical force fields used in Monte Carlo and molecular dynamics simulations typically employ effective pair potentials that include many-body effects in an average way. The increasing accuracy resulting from the development of current force fields raises the demand for the explicit inclusion of these many-body effects, particularly since the growth in computer power makes such approaches feasible. Here we present a simple model in which induced atomic dipoles are represented by charges on the atom itself plus neighboring atomic sites. Van Gunsteren and Berendsen[1] predicted that the inclusion of polarization in force fields would become possible by the end of the 1990s, and indeed, considerable advances in this field have been achieved. A rigorous theory for describing polarization has been given by Stone,[2] whose method gives accurate induced moments for small clusters of molecules[3,4] but is currently impractical for large biomolecular systems. A simpler approach assigns solely isotropic dipole polarizabilities to atoms and calculates the energy of the system from permanent point charges and induced point dipoles. The classical contribution by Vesely[5] introduces the theory required to perform the molecular dynamics simulations on systems with polarizable point dipoles. Several related models, primarily for water, have since been reported.[6−14] Rick and Berne have developed a different scheme[15] that accounts for polarization by atomic charges whose values depend on the molecular conformation and Coulomb interactions with the environment. This fluctuating charge model avoids the use of higher rank multipole moments (e.g., dipoles), and the electronegativity equalization theorem-based evaluation of the charges renders the calculation very fast. An extension of the method[16] introduces fluctuating dipoles, thus making the method capable of describing out of plane polarization of planar molecules. In the related chemical potential equalization model[17−19] it is also possible to represent the charge distribution by point charges only. Drude oscillator models for polarization[20] also use atomic charges, and the effect of polarization is accounted for by changes in the position of the charges;[21] such approaches are widely used in solid-state simulations.

In the present contribution, a novel method for describing polarization in classical force fields is described. This induced charge method invokes point charges only and is an approximation to the polarization model based on induced point dipoles. The point charges depend on the environment and in this sense our induced charge method is related to the fluctuating charge

* To whom correspondence should be addressed.
† Budapest University of Technology and Economics. Present address: Chinoin Rt., Tó 1-5, H-1045 Budapest, Hungary.
‡ University of Essex.

10.1021/jp0117967 CCC: $20.00
Published on Web 11/28/2001

model. Our method is based on the idea of representing a series of multipole moments by several lower rank multipole moments on neighboring sites.[22−25] Such a model was shown to be efficient in accounting for electrostatic interactions, and preliminary extensions to polarization using point charges have been described.[26,27] The method shares similarities with the approaches of Zhu et al.[28] and Sprik[29] but without the requirements for a regular geometry or a molecular dynamics implementation, respectively. In the present implementation the method has been systematically extended so that both the polarization energy and its derivatives can be determined.

In section 2, the established induced dipole model for polarization is summarized. In section 3 our new method using induced charge sets instead of induced dipoles is presented. The gradient of the electrostatic (including polarization) energy of the new model is given in section 4. In section 5, the relation between the two models and the approximations involved in the induced charge method together with its computational advantages are discussed. Some calculations on water and endothiapepsin that illustrate the ability of the method to account for polarization are presented in section 6, followed by conclusions in section 7.

2. Polarization with Induced Point Dipoles

Polarization in classical force fields can be treated by assigning point charges (q^{per}) and isotropic scalar polarizabilities (α) to the atoms.[6−8,12] Induced dipoles then arise due to the electrostatic field of the atomic charges and induced dipoles. The electrostatic energy of this charge + induced dipole set is given by

$$U = \frac{1}{2}\sum_I q_I^{\mathrm{per}} V_I = \frac{1}{2}\sum_{I,J} q_I^{\mathrm{per}} q_J^{\mathrm{per}} \frac{1}{r_{IJ}} + \frac{1}{2}\sum_{I,J} q_I^{\mathrm{per}} \left(\nabla \frac{1}{r_{IJ}}\right) \vec{\mu}_J^{\mathrm{ind}} \quad (1)$$

where V_I is the electrostatic potential at site I, $\vec{\mu}_J^{\mathrm{ind}}$ is the induced dipole at site J, and r_{IJ} is the length of the vector $\vec{r}_{IJ}$ pointing from site J to site I. Here (and below) vectors are marked by arrows (e.g., $\vec{\mu}_I^{\mathrm{ind}}$) and matrices are denoted by uppercase caligraphic letters (e.g., $\mathcal{X}$). In the case of double sums, the $I = J$ terms are omitted. Moreover, J skips sites neighboring to site I; depending on the actual force field, J may skip other sites such as the second neighbors of site I. This restriction on the summation indices is implicitly assumed throughout.

Equation 1 can be written in an alternative form

$$U = \frac{1}{2}\sum_{I,J} q_I^{\mathrm{per}} q_J^{\mathrm{per}} \frac{1}{r_{IJ}} + \sum_{I,J} q_I^{\mathrm{per}} \left(\nabla \frac{1}{r_{IJ}}\right) \vec{\mu}_J^{\mathrm{ind}} + \frac{1}{2}\sum_{I,J} \vec{\mu}_I^{\mathrm{ind}} \left(\nabla\nabla \frac{1}{r_{IJ}}\right) \vec{\mu}_J^{\mathrm{ind}} + U^{\mathrm{self}} \quad (2)$$

The first three terms describe the interactions of the charge + dipole set, and the last term, U^{self}, is the self-energy or polarization energy. This is the difference between the energy of the system (U of eqs 1 and 2) and the interaction energy of the charge + dipole set. U^{self} is interpreted as the energy required to create the induced dipoles;[30] it can be written in several alternative ways. Equation 2, with an appropriately chosen formula for U^{self} is an advantageous starting point for deriving the gradient of the energy,[5] which will be discussed in section 4.

To calculate induced dipoles, we need an expression for the electrostatic field, $\vec{\mathbf{F}}$, at point I

$$\vec{\mathbf{F}}_I = -\left[\sum_J q_J^{\mathrm{per}} \left(\nabla \frac{1}{r_{IJ}}\right) + \sum_J \left(\nabla\nabla \frac{1}{r_{IJ}}\right) \vec{\mu}_J^{\mathrm{ind}}\right] \quad (3)$$

The induced dipoles and the electric field are related by the equation

$$\vec{\mu}_I^{\mathrm{ind}} = \alpha_I \vec{\mathbf{F}}_I \qquad I = 1, 2, \ldots \quad (4)$$

The induced dipoles can be calculated from a system of linear equations derived from eqs 3 and 4. For a large ensemble with many variables it is more economical to calculate the induced dipoles in an iterative way. Starting with a set of charges and dipoles, the electrostatic field is calculated according to eq 3. This field is then used in eq 4 to calculate a new set of dipoles. The procedure is continued to self-consistency.

Making use of eqs 1−4, U^{self} can be written as

$$U^{\mathrm{self}} = \frac{1}{2}\sum_I \frac{1}{\alpha_I} \vec{\mu}_I^{\mathrm{ind}} \vec{\mu}_I^{\mathrm{ind}} \quad (5)$$

It should be noted that the above approach represents an approximate description of polarization. It neglects the anisotropic nature of polarizability and also neglects higher order polarizabilities and induced moments. Nevertheless, this is a reasonable approach to account for polarization and was successfully applied in molecular dynamics simulations;[6,8,11] it gives an improved description of the system albeit at increased computational cost.

3. Polarization with Induced Point Charges

The induced point charge method presented here is an approximation to the induced dipole model of section 2. Our aim is to find a compromise between the accuracy of the force field and the computational cost of evaluating polarization. The basic idea is that atomic point dipoles are represented by point charges on the neighboring atoms. It is appropriate to note here that a method[22−25] representing atomic point multipoles by lower rank moments on the atom itself and the neighboring atoms gives an efficient description of the static charge distribution of molecules. The method for deriving potential derived charges[31] can be considered as a special case of that scheme (see ref 22). The reproduction of induced atomic dipoles by point charges on neighboring atoms is illustrated using a pyramidal ammonia molecule as an example. The external field at the nitrogen position creates a dipole ($\vec{\mu}_I^{\mathrm{ind}}$) according to eq 4 of the induced dipole model. This dipole can be reproduced exactly by appropriately chosen point charges on the hydrogen positions.

$$\mathcal{X}_I \vec{\mathbf{p}}_I = \vec{\mu}_I \quad (6)$$

where $\vec{\mathbf{p}}_I$ is the array of the three hydrogen charges and $\mathcal{X}_I$ is a matrix composed of the three vectors pointing from the nitrogen to the hydrogen atoms

$$\mathcal{X}_I = (\vec{\mathbf{r}}_{\mathrm{H2N1}}, \vec{\mathbf{r}}_{\mathrm{H3N1}}, \vec{\mathbf{r}}_{\mathrm{H4N1}}) \quad (7)$$

To avoid introducing additional charge, a point charge opposite in sign and equal in magnitude to the sum of hydrogen charges is placed on the nitrogen atom. (This charge does not change the dipole as the vector from the nitrogen atom to the charge is zero.) Note, that the charge set (q_{N1}, q_{H2}, q_{H3}, q_{H4}) has the same zero and first multipole moments as those of the

model of section 2. The charges that reproduce the induced dipoles will be called induced charges.

Considering now the H2 atom, its induced dipole can be described by placing charges on the N1, H3, and H4 atoms. (When more than four atoms are available in the system, then a reasonable choice for the four charge centers includes those atoms that are nearest to the dipole and that are in the same molecule as the dipole itself. Such a choice tends to minimize higher rank multipole moments that are zero in the reference induced dipole approach.) Again, a charge is also placed on the H2 atom to neutralize the charge set. Continuing this procedure over all four induced atomic dipoles of the ammonia molecule gives rise to four partial induced charges ($p_{KK'}$, see below) on each atomic site and these may be summed to give the total induced charge (q_I^{ind}) on each atom. The total charge of each atom (q_I^{tot}) is obtained as the sum of the permanent charge and the total induced charge of the atom.

$$q_I^{\mathrm{tot}} = q_I^{\mathrm{per}} + q_I^{\mathrm{ind}} \tag{8}$$

q_I^{ind}, the (total) induced charge at site I, is given as

$$q_I^{\mathrm{ind}} = p_{II} + \sum_K \sum_{K' \in K} p_{KK'} \delta_{IK'} \tag{9}$$

with

$$p_{II} = -\sum_{I' \in I} p_{II'} \tag{10}$$

Here, the first index, I, of a partial induced charge $p_{II'}$ refers to the site of the dipole to be reproduced and the second index, I', refers to the site of the partial charge. Thus, the first term in eq 9, p_{II}, is the charge placed on atom I to balance the partial induced charges reproducing the dipole on I. According to eq 10, this is equal and opposite to the sum of charges on I', and $I' \in I$ designates that sites I' are involved in the reproduction of the dipole on I. The double sum in eq 9 includes those charges that are assigned to I to describe any dipole. (K is over all dipoles.) The dipole on K is reproduced by charges on K' and they contribute to q_I^{ind} if $I = K'$.

Having defined the basic quantities of the model, the equations used to calculate the energy and the induced charges are given below; their meaning is explained in section 5.

The electrostatic energy of a set of permanent and induced charges is

$$U = \frac{1}{2}\sum_I V_I q_I^{\mathrm{per}} = \frac{1}{2}\sum_{I,J} q_I^{\mathrm{tot}}\, q_J^{\mathrm{per}} \frac{1}{r_{IJ}} \tag{11}$$

(cf. eq 1).

Partial induced charges are given by the following relation

$$\vec{\mathbf{p}}_I = \alpha_I (\mathscr{T}_I^{+} \mathscr{T}_I)^{-1} \vec{\Delta}(\Phi_I) \tag{12}$$

where

$$\vec{\mathbf{p}}_I = \begin{pmatrix} p_{II'} \\ p_{II''} \\ p_{II'''} \end{pmatrix} \tag{13}$$

$$\vec{\Delta}(\Phi_I) = \begin{pmatrix} \Phi_I - \Phi_{I'} \\ \Phi_I - \Phi_{I''} \\ \Phi_I - \Phi_{I'''} \end{pmatrix} \tag{14}$$

and

$$\Phi_I - \Phi_{I'} = \sum_J \frac{q_J^{\mathrm{tot}}}{r_{IJ}} - \sum_J \frac{q_J^{\mathrm{tot}}}{r_{I'J}} \tag{15}$$

Thus, $\vec{\Delta}(\Phi_I)$ is an array whose first component is formed by the difference in electrostatic potentials (Φ) in positions I (central atom) and I' (neighboring atom). This array typically has three components, since the dipole moments on atom I can be reproduced by three charges placed at positions I', I'', and I'''. However, in certain cases three neighboring atoms are not available for induced charge positions. In these cases $\vec{\Delta}(\Phi_I)$ has less than three components and $\mathscr{T}_I$ is a rectangular matrix. The role of the matrix $(\mathscr{T}_I^{+}\mathscr{T}_I)^{-1}$ in eq 12 will be discussed in section 5. Equations 12−15, like eqs 3 and 4, can be solved iteratively.

Equations 11−15 specify the computational procedure for calculating induced charges and determine the energy of the set of permanent and induced charges.

4. Energy Gradient

To calculate forces, e.g., as required in a molecular dynamics simulation, we require the gradient of the energy; the evaluation of the gradient in the induced charge model is discussed in this section.

Equation 11 can be written in an alternative form

$$U = U^{\mathrm{int}} + U^{\mathrm{self}} = \frac{1}{2}\sum_{I,J} q_I^{\mathrm{tot}}\, q_J^{\mathrm{tot}} \frac{1}{r_{IJ}} + U^{\mathrm{self}} \tag{16}$$

where U^{self} is the polarization or self-energy. This is the difference between the energy of the system (U of eqs 11 and 16) and the interaction energy (U^{int}) of the set of total (permanent + induced) charges. Combining eqs 11 and 16 we obtain for U^{self}

$$U^{\mathrm{self}} = -\frac{1}{2}\sum_{I,J} \frac{1}{r_{IJ}} q_I^{\mathrm{ind}} q_J^{\mathrm{tot}} \tag{17}$$

Invoking eqs 9, 10, and 12, the last equation can be written as

$$U^{\mathrm{self}} = -\frac{1}{2}\sum_{I,J} q_I^{\mathrm{ind}} q_J^{\mathrm{tot}} \frac{1}{r_{IJ}} = -\frac{1}{2}\sum_I \Big(-\sum_{I' \in I} p_{II'} + \sum_K \sum_{K' \in K} p_{KK'} \delta_{IK'}\Big)\Phi_I = -\frac{1}{2}\sum_I \sum_{I' \in I} p_{II'}(\Phi_{I'} - \Phi_I) = \frac{1}{2}\sum_I \frac{1}{\alpha_I} \vec{\mathbf{p}}_I^{+} \mathscr{T}_I^{+}\, \mathscr{T}_I \vec{\mathbf{p}}_I \tag{18}$$

Note the analogy between the expression in the far right-hand side of this equation and that of eq 5. Substituting this expression for U^{self} into eq 16, one can show that

$$\frac{\partial U}{\partial p_{KK'}} = 0 \tag{19}$$

for any K and $K' \in K$. (Note that eq 19 is analogous to the condition $\partial U/\partial \vec{\mu}_K = 0$ from eq 2 with U^{self} from eq 5.[5])

Equation 19 can be derived as follows, with eq 20 coming from eq 16

$$\frac{\partial U}{\partial p_{KK'}} = \frac{\partial U^{\text{int}}}{\partial p_{KK'}} + \frac{\partial U^{\text{self}}}{\partial p_{KK'}} \tag{20}$$

Then

$$\frac{\partial U^{\text{int}}}{\partial p_{KK'}} = \sum_I \frac{\partial U^{\text{int}}}{\partial q_I^{\text{ind}}} \frac{\partial q_I^{\text{ind}}}{\partial p_{KK'}} \tag{21}$$

The two partial derivatives on the right-hand side can be written as

$$\frac{\partial U^{\text{int}}}{\partial q_I^{\text{ind}}} = \frac{\partial}{\partial q_I^{\text{ind}}} \frac{1}{2} \sum_{M,N} \frac{(q_M^{\text{per}} + q_M^{\text{ind}})(q_N^{\text{per}} + q_N^{\text{ind}})}{r_{MN}} = \sum_M \frac{q_M^{\text{per}} + q_M^{\text{ind}}}{r_{MI}} = \Phi_I \tag{22}$$

and

$$\frac{\partial q_I^{\text{ind}}}{\partial p_{KK'}} = \frac{\partial}{\partial p_{KK'}} \left(\sum_{I' \in I} -p_{II'} + \sum_L \sum_{L' \in L} p_{LL'} \delta_{IL'} \right) = -\delta_{KI} + \delta_{IK'} \tag{23}$$

Thus we can write

$$\frac{\partial U^{\text{int}}}{\partial p_{KK'}} = \sum_I \Phi_I (-\delta_{KI} + \delta_{IK'}) = \Phi_{K'} - \Phi_K \tag{24}$$

The second term on the right-hand side of eq 20 is

$$\frac{\partial}{\partial p_{KK'}} \frac{1}{2} \sum_I \frac{1}{\alpha_I} \vec{\mathbf{p}}_I^{+} \mathcal{T}_I^{+} \mathcal{T}_I \vec{\mathbf{p}}_I = \frac{1}{\alpha_K} (\vec{\mathcal{T}}_K^{+} \mathcal{T}_K \vec{\mathbf{p}}_{KK''})_{K'} \tag{25}$$

where the K' component of the array in brackets appears in the right-hand side. Making use of eq 12, the last derivative can easily be shown to equal the negative of the far right-hand side of eq 24. Thus eq 19 is derived.

The gradient of the energy in eq 16 with U^{self} from the far right-hand side of eq 18 is

$$\frac{\mathrm{d}U}{\mathrm{d}\vec{\mathbf{R}}_K} = \frac{\partial U}{\partial \vec{\mathbf{R}}_K} + \sum_I \sum_{I' \in I} \frac{\partial U}{\partial p_{II'}} \frac{\partial p_{II'}}{\partial \vec{\mathbf{R}}_K} \tag{26}$$

where $\vec{\mathbf{R}}_K$ is the vector pointing to the site of the (induced) charge K. The second term disappears according to eq 19. This represents a considerable simplification, since the gradients of $p_{II'}$ (derivatives of eq 12) do not have to be calculated. Thus the energy gradient can be written as

$$\frac{\mathrm{d}U}{\mathrm{d}\vec{\mathbf{R}}_K} = \frac{1}{2} \sum_{I,J} q_I^{\text{tot}} q_J^{\text{tot}} \frac{\mathrm{d}\frac{1}{r_{IJ}}}{\mathrm{d}\vec{\mathbf{R}}_K} + \sum_I \frac{1}{\alpha_I} \vec{\mathbf{p}}_I^{+} \mathcal{T}_I^{+} \frac{\mathrm{d}\mathcal{T}_I}{\mathrm{d}\vec{\mathbf{R}}_K} \vec{\mathbf{p}}_I \tag{27}$$

with

$$\frac{\mathrm{d}(\mathcal{T}_I)_{\xi' I'}}{\mathrm{d}R_{K\xi}} = \frac{\mathrm{d}(\vec{\mathbf{r}}_{I'I})_{\xi'}}{\mathrm{d}R_{K\xi}} = \frac{\mathrm{d}(R_{I'\xi'} - R_{I\xi'})}{\mathrm{d}R_{K\xi}} = \delta_{\xi\xi'} (\delta_{KI'} - \delta_{KI}) \tag{28}$$

where ξ and ξ' are any of the Cartesian components x, y, and z.

5. Comparison of the Induced Charge and Induced Dipole Models

5.1. Discussion of the Approximations. The model in section 3 is a consistent approximation to that of section 2, as shown in the following paragraphs.

First, the analogy between the formulas for induced charges, eq 12, and induced dipoles, eq 4, is discussed. Let us consider eq 29, which is equivalent with eq 4 in certain cases, as discussed below.

$$\mathcal{T}_I \vec{\mathbf{p}}_I = \alpha_I \mathcal{T}_I (\mathcal{T}_I^{+} \mathcal{T}_I)^{-1} \mathcal{T}_I^{+} \vec{\mathbf{F}}_I \tag{29}$$

The dipole, $\vec{\mu}^{\text{ind}}$, on the left-hand side of eq 4 is replaced by $\mathcal{T}_I \vec{\mathbf{p}}_I$. Typically $\vec{\mathbf{p}}_I$ has three components; the matrix $\mathcal{T}_I (\mathcal{T}_I^{+} \mathcal{T}_I)^{-1} \mathcal{T}_I^{+}$ is introduced to account for cases where less than three induced charges are available. (More precisely, this matrix plays a role when $\vec{\mathbf{r}}_{I'I}$, $\vec{\mathbf{r}}_{I''I}$, and $\vec{\mathbf{r}}_{I'''I}$ are not linearly independent.) In these cases, the dipole moment vector $\mathcal{T}_I \vec{\mathbf{p}}_I$ is restricted to the subspace spanned by the vectors $\vec{\mathbf{r}}_{I'I}$ and, therefore, only the component of the electrostatic field lying in that subspace is relevant for inducing a dipole moment. The matrix $\mathcal{T}_I (\mathcal{T}_I^{+} \mathcal{T}_I)^{-1} \mathcal{T}_I^{+}$ projects the electrostatic field, $\vec{\mathbf{F}}_I$, to this subspace. Note that this matrix is a unit matrix when the three vectors, $\vec{\mathbf{r}}_{I'I}$, $\vec{\mathbf{r}}_{I''I}$, and $\vec{\mathbf{r}}_{I'''I}$ are linearly independent. Equation 29 can be transformed into another form by expanding the electrostatic potential at position I' in a Taylor series

$$\Phi_{I'} = \Phi_I - \vec{\mathbf{r}}_{I'I} \vec{\mathbf{F}}_I + \ldots \tag{30}$$

Truncating this series at first-order we can write

$$\mathcal{T}_I^{+} \vec{\mathbf{F}}_I = \vec{\Delta}(\Phi_I) \tag{31}$$

with $\vec{\Delta}(\Phi_I)$ defined in eq 14.

Substituting eq 31 into eq 29 and performing simple algebraic manipulations gives eq 12. Thus it has been shown that eq 12 is an approximation to eq 4. These equations can be transformed into one another if induced charge centers adopt an appropriate geometry and if a Taylor expansion of the electrostatic potential is truncated at the first-order term.

The discussion on the analogy between the energy expressions of the two models involves showing that eq 11 is an approximation to eq 1. The former can be manipulated as follows

$$\frac{1}{2} \sum_{I,J} q_I^{\text{tot}} q_J^{\text{per}} \frac{1}{r_{IJ}} = \frac{1}{2} \sum_{I,J} q_I^{\text{per}} q_J^{\text{per}} \frac{1}{r_{IJ}} + \frac{1}{2} \sum_{I,J} q_I^{\text{ind}} q_J^{\text{per}} \frac{1}{r_{IJ}} \tag{32}$$

The first term is equal to that of eq 1. The second term can be written as

$$\frac{1}{2} \sum_{I,J} q_I^{\text{per}} q_J^{\text{ind}} \frac{1}{r_{IJ}} = \frac{1}{2} \sum_{I,J} q_I^{\text{per}} \frac{1}{r_{IJ}} \left[-\sum_{J' \in J} p_{JJ'} + \sum_K \sum_{K' \in K} p_{KK'} \delta_{JK'} \right] = \frac{1}{2} \sum_{I,J} \sum_{J' \in J} q_I^{\text{per}} p_{JJ'} \left[\frac{-1}{r_{IJ}} + \frac{1}{r_{IJ'}} \right] = \frac{1}{2} \sum_{I,J} q_I^{\text{per}} \left[\frac{1}{r_{IJJ'}} \sum_{J' \in J} (-p_{JJ'} + p_{JJ'}) + \nabla \frac{1}{r_{IJJ'}} \sum_{J' \in J} \vec{\mathbf{r}}_{J'J} p_{JJ'} + \ldots \right] \tag{33}$$

In the far right-hand side of eq 33, the first term in square brackets disappears, while the second term involves the dipole moment at site J. Thus, if we neglect terms above first order in eq 33, then we obtain that the second term of eq 32 corresponds to that of eq 1. The higher order terms in eq 33 contain higher order multipole moments and they represent the error of the present approximation with respect to the induced dipole model. While moments above dipole do not appear in the induced dipole model, they are nonzero in our induced charge model. This error decreases as the separation ($r_{J'J}$ with $J' \in J$ in the equation above) between the polarizable center and the induced charges

TABLE 1: Interaction Energies (kcal/mol) Calculated with Various Models

		interaction energy					
			with iteration			without iteration	
r(O−O) threshold	no. water molecules	permanent charges column 1[a]	induced dipoles[b] column 2	induced charges[c] column 3	induced charges with extra centers[c,d] column 4	induced dipoles[b] column 5	induced charges[c] column 6
0.0[e]	3363	−7348.00	−8810.31	−9379.29	−9438.90	−8570.32	−8937.80
2.6	3165	−6307.65	−7494.04	−7915.90	−7971.48	−7309.52	−7587.85
2.8	2031	−1870.39	−2116.48	−2140.76	−2163.73	−2091.20	−2107.43
3.0	1383	−374.17	−416.45	−407.53	−414.39	−414.73	−405.79
3.5	978	−95.97	−105.28	−102.15	−103.84	−105.25	−102.10
4.0	756	−63.94	−68.09	−67.00	−67.64	−68.07	−66.98
5.0	447	−16.77	−17.55	−17.32	−17.45	−17.55	−17.31
water dimer (Figure 2a)		−5.24	−5.83	−5.91	−5.95		
water dimer (Figure 2b)		−1.65	−2.12	−1.81	−2.00		
Endothiapepsin(−)[f]		−53.74	−62.16	−59.75	−61.68		
Endothiapepsin(2−)[g]		−44.38	−47.97	−46.95	−47.43		

[a] Column numbers are used in the text to reference table entries. [b] Energy of permanent charges + induced dipoles. [c] Energy of permanent charges + induced charges. [d] Induced dipoles are described with three charge centers: the two other atoms in the molecule and a third one separated by 0.1 Å from the O atom and above the plane of the water molecule. [e] Snapshot from water droplet simulation; smallest separation between oxygen atoms is shown in ångströms (see text). [f] Endothiapepsin fragment with one charged and one uncharged aspartate residue. [g] Endothiapepsin fragment with two charged aspartate residues.

decreases and also decreases with increasing intermolecular separations (r_{IJ}). One can show in a similar manner that eq 16 is an approximation to eq 2.

The above derivations show that the induced dipole model reduces to the induced charge model if terms above first order are neglected in a multipolar expansion. Furthermore, the geometrical arrangement of the induced charge centers has to satisfy a certain criterion so that charges are able to represent point dipoles.

5.2. Polarization Models without Iteration. A significant part of the computational work in both the induced charge and induced dipole models is the iterative determination of the induced moments. This can be avoided by approaches in which the induced moments arise solely from the polarizing effect of permanent charges and the polarizing effect of the induced moments are not included. Such a model for induced dipoles was proposed by Straatsma and McCammon[7,34] as an economical way to calculate the major part of the polarization energy.

In the induced dipole approach, a model without iteration can be obtained by omitting the second term on the right-hand side of eq 3 and similar approximations have to be applied to derive eq 5 and to obtain $\partial U/\partial \vec{\mu}_I^{\text{ind}} = 0$.

In the induced charge model, iteration is avoided by replacing q_I^{tot} by q_I^{per} on the right-hand side of eq 15. Similar approximations are needed in eq 18 to obtain the formula of self-energy and in the last step of eq 22 to derive $\partial U/\partial p_{KK'} = 0$ (eq 19).

5.3. Computational Work Associated with the Models. The computational advantage of the induced charge model over the induced dipole model is that in the induced charge model no interaction tensors between charges and dipoles and between dipoles and dipoles are needed. This simplifies both the evaluation of the interaction energy (compare eqs 11 and 1) and the iterative determination of induced charges (compare eqs 12−15 and 3 and 4). A similar advantage applies to the calculation of energy derivatives. On the other hand, the appearance of matrix $\mathcal{T}$ and, in particular, of $(\mathcal{T}^+\mathcal{T})^{-1}$ in the induced charge model represents a complication not present in the induced dipole model. However, these matrices belong to induced sites and so the associated computational work is proportional to the number of induced sites. The extra work in the induced dipole model comes from the evaluation of interatomic interaction tensors and so the associated computational work is expected to increase faster with increasing system size. Calculations presented in the next section support this expectation.

To speed up the calculation in the induced charge model, it is advantageous if, in the course of the iterative determination of induced charges, the matrices $(\mathcal{T}^+\mathcal{T})^{-1}$ are evaluated in the first iterative cycle and then are stored and recalled in the subsequent cycles. As $(\mathcal{T}^+\mathcal{T})$ contains the dot products of interatomic vectors, these matrices do not change for rigid molecules and can be used throughout the simulation. Even if the geometry remains only approximately constant, as expected in the simulation of certain systems near to equilibrium, the use of constant or occasionally updated $(\mathcal{T}^+\mathcal{T})$ matrices may be an acceptable approximation.

6. Numerical Examples and Discussion

To test the capability of the method, some comparisons between applications of the induced charge and induced dipole models are presented below.

In the first example, we analyze a snapshot of a molecular dynamics simulation of an equilibrated spherical water droplet of radius 20 Å containing 3363 TIP3P[32] water molecules. The interaction energy of a snapshot of the system generated using the TIP3P charges was evaluated using a new set of permanent charges (see below) together with a permanent charge + induced dipole and a permanent charge + induced charge system. The latter two models were applied with and without iteration. In addition to calculating the total electrostatic + polarization energy of the whole snapshot configuration, further systems were generated by omitting from the calculations those water molecules whose oxygen atoms lie within a given r(O−O) threshold separation. In this way we were able to study both the importance of the polarization energy at different intermolecular separations and the capability of the approximations to account for the polarization energy in the various systems.

The permanent atomic charges were chosen so that the experimental vacuum dipole moment of water (1.85 D) was reproduced. Thus $q_O = 0.656\ e^-$ was used instead of the TIP3P charges ($q_O = 0.834\ e^-$, $\mu_{H_2O} = 2.35$ D). The atomic polarizability values were taken from ref 33. The results in Table 1 show that error caused by the neglect of polarization (difference between columns 2 and 1) is greatly reduced by approximating

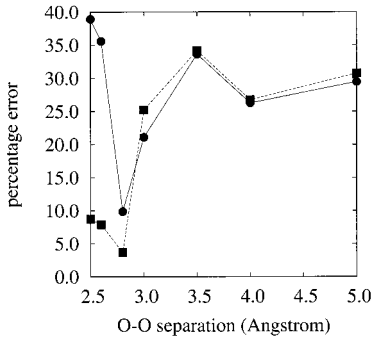

Figure 1. Relative error of the induced charge model with (●) and without (■) iterations for several hollow water droplets generated by omitting from the calculations those water molecules whose oxygen atoms lie within a given *r*(O−O) threshold separation.

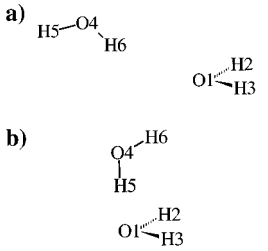

Figure 2. (a) Schematic representation of a water dimer near its equilibrium arrangement. (b) Schematic representation of a water dimer poorly described by the induced charge model. The polarization effect of the electrostatic field arising from the upper molecule and perpendicular to the plane of the lower molecule cannot be accounted for by distributed atomic charges.

the polarization contribution using the induced charge model (the difference between columns 3 and 2). The graph of the error of the induced charge model (column 3 − column 2) as the percentage of the error corresponding to the complete neglect of polarization (column 2 − column 1) against *r*(O−O) exhibits a minimum (Figure 1). The observation that the percentage error generally increases with distance above ∼2.8 Å (even though the absolute error generally decreases) is surprising, since the induced charge model is expected to perform better at larger intermolecular separations. The behavior of the curve in Figure 1 can be explained by considering the structure of liquid water. The minimum error is observed at the *r*(O−O) separation of 2.8 Å; this corresponds approximately to an optimal hydrogen bond. These interactions dominate in the system, as they correspond to a water dimer near to its equilibrium geometry (Figure 2a). The induced charge model performs well for such an interaction (see the Figure 2a dimer in Table 1 and the discussion below). When these interactions are removed from the water droplet by omitting from the calculations (of both field and energy) molecules closer than a given *r*(O−O) intermolecular separation, the relative error of the induced charge model increases. In water droplets, a variety of relative water molecule orientations occur and some of them are described less efficiently by the induced charge model. A particularly disadvantageous arrangement in this respect is shown in Figure 2b. Note that the energy lowering due to induction has a similar magnitude in both water dimers; for Figure 2a this is −0.59 kcal/mol and for Figure 2b it is −0.47 kcal/mol (difference between columns 1 and 2 of Table 1). However, in the latter case (Figure 2b), an important electrostatic field perpendicular to the plane of the lower molecule arises and the dipole induced cannot be described by distributed atomic charges on sites within the plane. In such situations, the induced charge model is only able to recover a small fraction of the polarization energy (−0.16 kcal/mol for Figure 2b vs −0.67 kcal/mol for Figure 2a; difference between columns 1 and 3 in Table 1).

To test the importance of the out of plane polarization, a further center for induced charge is added to each water molecule. This center is placed at 0.1 Å separation from the O atom so that the vector pointing from the O atom to this center is perpendicular to the plane of the molecule. Comparing the data in columns 2−4 of Table 1 shows that for the water dimer of Figure 2b, the inclusion of out-of-plane charge centers results in excellent reproduction of the reference energy of the induced dipoles. On the other hand, no improvement in the energy of the water dimer of Figure 2a is observed. In fact, the energy obtained without extra centers is fortuitously closer to the reference energy of the induced dipoles. The overestimation of the polarization energy with extra charge centers also appears in the energy of water droplets containing primarily these types of interactions (molecules with *r*(O−O) separation 0.0−3.0 Å retained, first three rows in Table 1).

The error in the polarization energy of the dimer of Figure 2a obtained with out-of-plane induced charge centers is slightly over 0.1 kcal/mol (difference between columns 4 and 2 of Table 1; about 14% of the polarization energy), suggesting that this is the magnitude of the intrinsic error of the induced charge model for this system. The observation that the representation of induced dipoles by induced charges is less satisfactory for close molecules is probably partly a consequence of the increased importance of higher rank moments in the interactions. In the induced charge model, the multipole moments of the charge sets that are higher than first rank (i.e., higher than dipole) are not zero and their interactions contribute to the calculated energy. The poorer results for close molecules are in line with the former observation that the representation of the static charge distribution of van der Waals complexes by point charges (even with potential derived charges) is an unsatisfactory approximation regarding its ability to describe correctly the geometrical and energetic aspects of the intermolecular interactions of such systems.[25]

The induced charge approximation is based on the reproduction of the induced dipoles by induced charges. This is demonstrated by data in Table 2. The atomic dipoles of the induced charge sets are shown for the oxygen atoms of the water dimers of Figure 2a,b. They were calculated with atomic centers only and also with atomic plus out-of-plane centers. The dipoles of the induced dipole model are also shown for reference. It is expected that dipoles of induced charges differ from the reference data owing to the approximate representation of the inducing field, which is calculated from potential differences using eq 12. We expect this effect to be more pronounced for close molecules. At this point it is worth emphasizing that the replacement of $\mathcal{X}_I^+\vec{\mathbf{F}}_I$ by $\vec{\Delta}(\Phi_I)$ (cf. eq 31) is not an extra approximation, rather it is an integral part of the induced charge model so that the model is equivalent with the induced dipole approach up to the first order of a multipolar expansion of the interactions. A further cause for the difference in dipole moments is a geometrical restriction. The O1, H2, and H3 atoms of both dimers are in the *xz* plane. Accordingly, there is no dipole in the *y* direction in the induced charge model when only atomic centers are used. On the other hand, the *y* components of the dipole moments are nonzero in the induced dipole model. As the *y* component is smaller in the dimer of Figure 2a, the induced charge model performs better in this case (cf. Table 1 and discussion above). When out-of-plane charge centers are present, then dipole moments in this direction also appear in

TABLE 2: Induced Atomic Dipole Moment Components (Debye) Calculated with the Induced Charge and Induced Dipole Models for the Oxygen Atoms of Water Dimers in Figure 2a,b[a]

	dipoles of induced charges[b]								
	atomic centers only[c]			atomic + out-of-plane centers			induced dipoles[d]		
atom	x	y	z	x	y	z	x	y	z
dimer of Figure 2a									
O1	0.106(0.090)	0.000(0.000)	0.000	0.106	−0.046	0.000	0.119	−0.041	0.000
O4	0.113(0.104)	−0.083(−0.077)	0.000	0.115	−0.084	0.002	0.059	−0.048	0.000
dimer of Figure 2b									
O1	0.033(0.029)	0.000(0.000)	0.000	0.034	−0.112	0.000	−0.020	−0.118	0.000
O4	−0.021(−0.020)	−0.073(−0.071)	0.000	−0.020	−0.083	−0.001	−0.035	−0.038	0.000

[a] The *x* axis in Figure 2 is horizontal, the *y* axis is vertical, and the *z* axis is out of the paper. [b] Dipoles are calculated from partial induced charges according to eq 6. [c] Dipoles of charges obtained without iteration are shown in parentheses. z components are zero by symmetry. [d] Dipoles from the induced dipole model.

TABLE 3: Computational Time (s) for Various Models and Systems[a]

		computational time with gradients				
			with iteration		without iteration	
r(O−O) threshold	no. water molecules	permanent charges	induced dipoles[b]	induced charges[c]	induced dipoles[b]	induced charges[c]
0.0[d]	3363	5.83	61.55	27.75	19.25	8.65
2.6	3165	5.12	49.52	21.65	17.06	7.57
2.8	2031	1.97	18.33	7.05	7.01	2.85
3.0	1383	0.88	7.54	2.65	3.25	1.26
3.5	978	0.42	3.78	1.08	1.63	0.60
4.0	756	0.24	1.96	0.50	0.97	0.34
5.0	447	0.08	0.68	0.17	0.34	0.11

[a] Energies and gradients are evaluated. [b] Energy of permanent charges + induced dipoles. [c] Energy of permanent charges + induced charges. [d] Snapshot from water droplet simulation; smallest separation between oxygen atoms is shown in ångströms (see text).

the induced charge model. Note that in this case small *z* moments arise in the induced charge model. These *z* components are zero by symmetry in the induced dipole model. However, the asymmetrical introduction of the out-of-plane charge centers allows the emergence of this dipole moment component in the induced charge model.

It is worth mentioning that in the water droplet corresponding to the first numerical row of Table 1, the charges, $q_O^{per} = 0.656$ e^-, assigned to the model increase in average to $q_O^{tot} = 0.821$-($\pm$0.043) e^- as a result of polarization. This value is near the charge (0.834 e^-) in the TIP3P model,[32] whose geometry was adopted in our calculations. As the TIP3P charges were determined to optimally describe specific physical properties of water, the above finding suggests that the induced charge model with appropriate atomic polarizabilities captures the essence of the physical phenomena of polarization.

The computational work associated with the polarization calculations is dominated by the iterative determination of the induced moments. In our naive implementation, one iteration cycle of the induced charge calculation is 2−4 times faster than one iteration of the induced dipole calculation. The number of cycles in the iteration is between 2 and 8, being higher when close molecules are involved. When interaction energies with iterated induced charges are calculated together with energy gradients, then the gain is still 2−4-fold with respect to the same calculation with iterated induced dipoles (Table 3).

The last two columns of Table 1 show energies obtained with induced moments calculated without iteration. In other words, the induced charges/dipoles are generated by permanent charges only. Energies obtained without iterating the moments tend to be slightly smaller in absolute value but they are close to the energies obtained with iterated moments. Interestingly, for systems with close molecules (r(O−O) = 0.0−2.8 Å), energies calculated with induced charges without iteration (column 6) tend to be closer to the reference values (energy of iterated induced dipoles in column 2) than energies obtained with iterated induced charges (column 3). This is illustrated also in Figure 1. The better performance of the charge set obtained without iteration is owing to the smaller magnitude of these charges. They represent a less polar charge distribution and generate smaller multipole moments (see Table 2 for dipoles). As moments above the dipole are zero in the reference-induced dipole model, the reduction of these moments by omitting iteration improves the agreement with reference.

It is also worth noting that energies of the induced charge and induced dipole models are closer when no iteration is performed (cf. columns 5 and 6 vs 2 and 3).

Our results suggest that the use of moments without iteration is an appealing approximation, particularly in the induced charge approach where it can lead to a 7-fold reduction in the CPU time but also in the induced dipole approach (Table 3).

In another example, the polarization in the active site of endothiapepsin was investigated. Endothiapepsin is an aspartic protease whose active site contains two aspartate residues. In a complex formed with the H-261 inhibitor, two oxygen atoms of the aspartate residues are separated by approximately 3 Å.[35−37] It was found by Gomez and Freire[38] that one of the aspartate residues is protonated, and this, together with an extended hydrogen bonded network that also involves the inhibitor, stabilizes the arrangement of neighboring aspartate residues. A fragment of the X-ray structure was cut off (Figure 3) and hydrogen atoms were added to optimize hydrogen bond interactions. The interaction energy was calculated using STO-3G potential derived charges taken from the amber force field[39] (which were used as permanent charges) and polarizabilities taken from ref 33. Interaction energies using both the induced dipole and the induced charge models are shown in the penultimate row of Table 1. Taking the energy of the induced dipole moment model as the reference value, the induced charge model returns 96% of the total energy (cf. columns 2 and 3) and 72% of the polarization energy (cf. columns 2 and 1 vs 3 and 1), compared to 86% (cf. columns 1 and 2) and 0%,

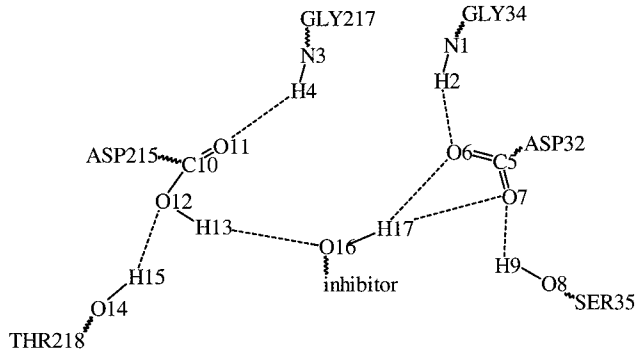

Figure 3. Schematic representation of the active site of the endothiapepsin−H-261 complex with atom numbering.

respectively, for the permanent charge model. The method performs better when changes in polarization energy are compared. Thus the results for a separate calculation in which both aspartate residues were charged are given in the last row of Table 1. Comparing the results obtained for this system with those of the system with one charged aspartate residue shows that 90% of the change in the polarization energy as calculated by the induced dipole method (14.19 kcal/mol; difference of last two rows in column 2) was recovered by the induced charge method (12.80 kcal/mol; difference of last two rows in column 3).

The difference in energies stems from the following factors. As discussed in section 5, the induced dipole model reduces to the induced charge model if terms above first order of a multipolar expansion of the interactions are neglected. The approximation manifests itself in an approximate representation of the inducing field (cf. eqs 12 and 31) and in an emergence of nonzero multipole moments above dipole (cf. eq 33). A further factor affecting the value of the dipole moments generated by the induced charges is geometric in nature and also appeared in the water−water interactions. It arises when the arrangement of charge sites does not allow for the reproduction of certain components of an induced dipole, as in Figure 2b. This effect is clearly present here since the endothiapepsin fragment considered involves small two- and three-atom molecular fragments. It is worth noting that complementing the molecular fragments with further centers in the same residue may remedy this geometrical constraint by making available further centers in appropriate positions. However, there is a limit to the involvement of centers since they cannot be further away than any interacting nonbonded atom. In fact, it is desirable that charge sites be as close to the dipole center as possible; otherwise, the nonzero higher moments have a nonnegligible effect on the interaction. A possible remedy to the geometric restriction, as in the case of water molecules, is the inclusion of extra induced charge centers, making it possible to account for out-of-plane polarization. Indeed, as shown in the fourth column of Table 1, the energy obtained with extra charges centers is in excellent agreement with the energy of the induced dipoles.

The induced charge method realizes a representation of the zero charge and the induced dipole moment (or a subset of the dipole moment's components). In a related method, a distributed multipole series representing the static charge distribution of a molecule is reproduced by lower rank moments on neighboring sites.[22−25] These lower rank moments are obtained in a fitting procedure such that the original multipole moments are reproduced as well as possible. This fitting includes the original multipole moments up to rank 6−8 but lower weights are used in the reproduction of the higher rank moments in line with their decreasing importance. It was found that fitted moments, typically up to dipoles, are able to describe accurately the electrostatic interaction of van der Waals complexes.[25] The good performance of these fitted moments, even at short intermolecular separations, arises because the higher rank original moments, which are increasingly important at short intermolecular separations, are also approximately reproduced by the lower rank fitted moments. In the induced charge model on the other hand, there is no attempt to reproduce moments above dipole, and this represents an error that becomes more important with decreasing intermolecular separations. The reproduction of higher rank moments is not straightforward in the induced charge model. In general, point charges are placed on the site of the dipole and on three neighboring sites so that the four charges are able to reproduce the zero total charge and the three components of the dipole. The inclusion of further charge centers would make it possible to reproduce higher rank moments. However, charge centers have to be closer than any interacting site to ensure the validity of the multipole expansion that the method is based on. This is generally not satisfied with the inclusion of second nearest neighbors. Another possibility is to adopt a fitting scheme, as in the calculation of low rank fitted moments for the static charge distribution, but this is hindered by the need to evaluate the positional derivatives required in a molecular dynamics implementation. On the other hand, such an approach may be useful in a Monte Carlo simulation.

Pair potentials with atomic point charges are not well suited to an accurate reproduction of the experimental properties of molecular dimers. In particular, the orientation dependence of the interaction energy is purely described (see, e.g., refs 13, 25, 40, and 41) and the introduction of dipole polarizability is not expected to considerably improve the situation. On the other hand, simple point charge models are able to describe the bulk properties of water remarkably well. Various TIP[32] and SPC[12,42] models are intensively used in molecular dynamics and Monte Carlo simulations as they represent a good compromise between accuracy and computational requirements. Therefore, as a further test of the ability of the induced charge model, we investigated whether improvement in predicting the properties of water can be achieved by combining the model with a TIP3P type water potential.

The induced charge model was implemented in the TINKER[43] molecular dynamics code. NpT simulations under periodic boundary conditions were performed for a cubic box of 216 water molecules coupled to an external heat and pressure bath[47] at 298 K and 1 atm. The TIP3P[32] water geometry was adopted. Bond lengths and angles were held fixed using SHAKE.[44] The permanent atomic charges were set so that they reproduce the experimental dipole moment in a vacuum ($q_O = -0.656\ e^-$, $\mu = 1.85$ D). The experimental dipole polarizability of water, 1.445 Å^3,[45] was assigned to the oxygen atom. The parameters of the Lennard-Jones 6-12 potential were adjusted. This model will be referred to as TIP3P−IC.

When simulations with TIP3P Lennard-Jones parameters were performed, the "polarization catastrophe", i.e., the increase in the absolute value of the interaction energy due to infinite mutual polarization of nearby centers, was occasionally observed. The induced charge model is more susceptible to such events than the induced dipole model since a dipole induced on an oxygen atom is described by charges on the bonded hydrogen atoms and these may approach within 2 Å of neighboring polarizable oxygen sites. A possible way to avoid the "polarization catastrophe" is to increase the repulsion part of the interaction potential. We followed, however, another route and calculated

TABLE 4: Parameters of Water Simulations

no. of molecules		216
cutoff radius, Å		9.0
r_{OH}, Å		0.9572
∠HOH, Å		104.52
	TIP3P[a]	TIP3P−IC[b]
α_O, Å^3		1.445[c]
T, K	298(±4)	298(±5)
press., atm	10(±553)	0(±541)
$10^{-3}A$, kcalÅ^{12}/mol	582.0	748.6
C, (kcal Å^6)/mol	595.0	723.9
q_O^{perm}, e	−0.834	−0.656
μ^{perm}, D	2.35	1.85[d]
time step, fs	1	1
equillibration, ps	40	40
data collection, ps	60	60

[a] See ref 32. [b] Model with induced charges. [c] Experimental value from ref 45. [d] Experimental dipole moment in a vacuum.

induced charges without iteration. As discussed above, the use of noniterative induced charges is advantageous for both decreasing the required computation work and also for yielding good interaction energies. In the context of molecular dynamics it has a further advantage. While induced charges originating from distant molecules are well described by the noniterative scheme, the exaggeration of charges leading to the "polarization catastrophe" is the result of iteration. Thus, the noniterative calculation of induced charges leads to an interaction potential that is similar to the potential of iterated induced charges at larger intermolecular separations while it gives a reduced attraction at small separations.

The parameters of molecular dynamics simulations are shown in Table 4 and predicted properties are presented in Table 5. Results of the TIP3P model and those of the induced charge model are shown together with two other polarizable water models and the experimental values. Density, internal energy and diffusion constants of the TIP3P−IC are all superior to their TIP3P counterparts and they are similar in quality with other polarizable water models. Considering the O−O radial distribution function (Figure 4), again TIP3P−IC represents a considerable improvement over the entire range of the O−O separation. The improvement is particularly notable above the first minimum of the curve, the region where experimental functions are more unanimous[46] and show more pronounced structure than TIP3P.

For a correct appreciation of the performance of the TIP3P−IC model, it has to be emphasized that only two parameters, those of the Lennard-Jones potential were adjusted, while geometrical parameters, atomic charges and polarizabilities were taken to conform experimental values. This is in contrast to the derivation of the nonpolarizable TIP3P model where the atomic charge is an additional adjustable parameter. Owing to the more physical nature of the TIP3P−IC model, it is expected to be applicable over a wider range of conditions and also in inhomogeneous systems.

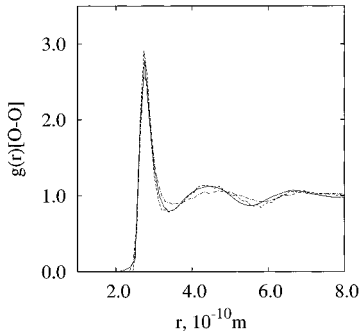

Figure 4. Radial O−O distribution function for the TIP3P−IC model (dashed line), for the TIP3P model (dashed−dotted line), and from experiment[48] (solid line).

7. Conclusion

The induced charge model presented here is a consistent method for describing polarization by distributed atomic charges. The model uses permanent atomic charges and isotropic atomic polarizabilities to derive induced charges. These charges approximate the effect of induced dipoles, which are more commonly used to account for polarization. Numerical studies suggest that the error caused by completely neglecting polarization is substantially reduced by using the induced charge model. The computational cost of the induced charge model is a quarter to a half of the induced dipole model both with and without gradient evaluation. It was found that restricting the calculation to the polarization arising from the permanent charges only, i.e., omitting iteration, considerably decreases the computation required (up to 7-fold gain in efficiency) and results in similar polarization energies as calculations with full iteration. It should be emphasized, however, that timings are highly dependent on the effectiveness of the implementation.

Induced charges were successfully introduced in the TIP3P water model, resulting in a polarizable water potential that significantly outperforms TIP3P. These results suggest that an effective polarizable force field can be derived by combining the induced charge model with further energy components.

The limitations of the induced charge model come from the following sources. The inducing field is approximated by an expression containing finite differences of the electrostatic potential. Moreover, besides the accurate representation of the zero charge and the three components of the induced dipole moment, distributed charges generate nonzero higher moments that should be zero if we consider the induced dipole model as the benchmark. A further limitation is that in certain cases some components of the induced dipole moments cannot be represented by distributed charges on neighboring sites simply because of the geometrical arrangements of the atoms. A typical example is the water molecule, in which dipole moments perpendicular to the molecular plane cannot be accounted for by distributed atomic charges. This limitation can be overcome

TABLE 5: Predicted Properties of Liquid Water with Various Water Models[a]

	TIP3P[b]	PCP[c]	SPC-pol-2[d]	TIP4P-pol-3[d]	TIP3P−IC[e]	experimental
density, g/cm^3	0.973_7[f]	0.997	1.057_3	0.995_2	0.993_8	0.997[g]
diff.const., 10^{-9} m^2 s^{-1}	4.6_1	2.6			2.0	2.3[h]
q_O^{tot}, e	−0.834				-0.946_4	
μ^{tot}, D	2.35	2.51	2.43	2.45	2.67_1[i]	
E^{pot}, kcal/mol	-9.60_6[j]	−9.89[k]	−9.94[k]	−9.82[10]	-10.15_{11}	−10.0 to −10.5[b]
E^{self}, kcal/mol					3.61_8	

[a] Uncertainty in the last figure, when available, is shown as subsript. [b] See ref 32. [c] See ref 13. [d] See ref 14. [e] Model with induced charges. [f] 0.982 g/cm^3 is reported in ref 32. [g] See ref 50. [h] See ref 49. [i] According to recent high level quantum chemical calculations[51] the average dipole moment of water in liquid is 2.65 D. [j] −9.86 kJ/mol is reported in ref 32. [k] A conversion factor of 4.184 was used between kJ/mol and kcal/mol.

by the introduction of off-atomic induced charge centers placed out of the plane of the molecule. In certain cases, the introduction of such centers was shown to improve interaction energies considerably (Figure 2b, Table 1). On the other hand, new centers are unnecessary when the major component of the inducing field is in the molecular plane, e.g., for systems containing hydrogen-bonded water molecules in an energetically favorable arrangement shown in Figure 2a.

It should be noted that the above limitations seem to be generally valid for any distributed charge model independent of the how the charges were generated. In particular, the limited capability of distributed charge models to account for polarization (and, in general, electrostatic interactions) of molecules near to the sum of their van der Waals radii should be emphasized.

On the other hand, the induced charge model provides a systematic way to approximate induced dipoles. The induced charge and induced dipole models are equivalent up to the first order of a multipolar expansion of the interactions and, in this respect, the induced charge model is the best possible distributed point charge approximation. The model has a sound physical basis and is consistent with methods describing electrostatics with effective charges, i.e., with charges that include the effect of higher rank multipole moments. Thus the model provides a parameter-free general description of intermolecular polarization within the above limitations.

Acknowledgment. This work was partly supported by the National Fund for Scientific Research (OTKA/T32032). G.G.F. acknowledges receipt of a Bolyai János grant. We thank Drs. L. Pusztai and G. Tóth for helpful discussions on the interpretation of experimental data for liquid water.

References and Notes

(1) van Gunsteren, W. F.; Berendsen, H. J. C. *Angew. Chem., Int. Ed. Engl.* **1990**, *29*, 992.
(2) Stone, A. J. *J. Mol. Phys.* **1985**, *56*, 1065.
(3) Buckingham, A. D.; Fowler, P. W.; Stone, A. J. *Int. Rev. Chem.* **1986**, *5*, 107.
(4) Fowler, P. W.; Stone, A. J. *J. Phys. Chem.* **1987**, *91*, 509.
(5) Vesely, F. J. *J. Comput. Phys.* **1977**, *24*, 361.
(6) Wang, J.; Jordan, P. C. *J. Chem. Phys.* **1990**, *93*, 2762.
(7) Straatsma, T. P.; McCammon, J. A. *Mol. Simulation* **1990**, *5*, 181.
(8) Ramnayaran, K.; Rao, B. G.; Singh, U. C. *J. Chem. Phys.* **1990**, *92*, 7057.
(9) Ahlström, P.; Wallqvist, A.; Engström, S.; Jönsson, Bo. *Mol. Phys.* **1989**, *68*, 563.
(10) Sprik, M.; Klein, M. L. *J. Chem. Phys.* **1988**, *89*, 7556.
(11) Caldwell, J.; Dang, L. X.; Kollman, P. A. *J. Am. Chem. Soc.* **1990**, *112*, 9144.
(12) Berendsen, H. J. C.; Grigera, J. R.; Straatsma, T. P. *J. Chem. Phys.* **1987**, *91*, 6269.
(13) Svishchev, I. M.; Kusalik, P. G.; Wang, J.; Boyd, R. J. *J. Chem. Phys.* **1996**, *105*, 4742.
(14) Chen, B.; Xing, J.; Siepmann, J. I. *J. Phys. Chem. B* **2000**, *104*, 2391.
(15) Rick, S. W.; Berne, B. J. *J. Am. Chem. Soc.* **1996**, *118*, 672.
(16) Stern, H. A.; Kaminski, G. A.; Banks, J. L.; Zhou. R.; Berne, B. J.; Friesner, R. A. *J. Phys. Chem. B* **1999**, *103*, 4730.
(17) Itsikowitz, P.; Berkowitz, M. L. *J. Phys. Chem. A* **1997**, *101*, 5687.
(18) York, D. M.; Yang, W. *J. Chem. Phys.* **1996**, *104*, 159.
(19) Bret, C.; Field, M. J.; Hemmingsen, L. *Mol. Phys.* **2000**, *98*, 751.
(20) Hirschfelder, J. O.; Curtiss, L.; Bird, R. B. *Molecular Theory of Gases and Liquids*; Wiley: New York, 1954..
(21) Dick, B. G.; Overhauser, A. W. *Phys. Rev.* **1958**, *112*, 90.
(22) Ferenczy, G. G. *J. Comput. Chem.* **1991**, *12*, 913.
(23) Chipot, C.; Ángyán, J. G.; Ferenczy, G. G.; Scheraga, H. A. *J. Phys. Chem.* **1993**, *97*, 6628.
(24) Winn, P. J.; Ferenczy, G. G.; Reynolds, C. A. *J. Phys. Chem. A* **1997**, *101*, 5437.
(25) Ferenczy, G. G.; Winn, P. J.; Reynolds, C. A. *J. Phys. Chem. A* **1997**, *101*, 5446.
(26) Gooding, S. R.; Winn, P. J.; Maurer, R. I.; Ferenczy, G. G.; Miller, J. R.; Harris, J. E.; Griffiths, D. V.; Reynolds, C. A. *J. Comput. Chem.* **2000**, *21*, 478.
(27) Winn, P. J.; Ferenczy, G. G.; Reynolds, C. *J. Comput. Chem.* **1999**, *20*, 704.
(28) Zhu, S.-B.; Yao, S.; Zhu, J.-B.; Singh, S.; Robinson, G. W. *J. Phys. Chem.* **1991**, *95*, 6211.
(29) Sprik, M. *J. Phys. Chem.* **1991**, *95*, 2283.
(30) Böttcher, C. J. F *Theory of Electric Polarization*; Elsevier: Amsterdam, 1973; Vol. 1, p 110.
(31) Cox S. R.; Williams, D. E. *J. Comput. Chem.* **1981**, *2*, 304.
(32) Jorgensen, W. L.; Chandrasekhar, J.; Madura, J. D.; Impey, R. W.; Klein, M. L. *J. Chem. Phys.* **1983**, *79*, 926.
(33) Applequist, J.; Carl, J. R.; Kwok-Keung, F *J. Am. Chem. Soc.* **1972**, *94*, 2952.
(34) Straatsma, T. P.; McCammon, J. A. *Chem. Phys. Lett.* **1990**, *167*, 252.
(35) Berman, H. M.; Westbrook, J.; Feng, Z.; Gilliland, G.; Bhat, T. N.; Weissig, H.; Shindyalov, I. N.; Bourne, P. E. *Nucleic Acids Research*; The Protein Data Bank, **2000**, pp 235−242.
(36) Veerapandian, B.; Cooper, J. B.; Szelke, M.; Blundell, T. L. Protein Data Bank, Entry 2ER7 1990.
(37) Veerapandian, B.; Cooper, J. B.; Sali, M. A.; Blundell, T. L. *J. Mol. Biol.* **1991**, *216*, 1017.
(38) Gomez, J.; Freire, E. *J. Mol. Biol.* **1995**, *252*, 337.
(39) Weiner, S. J.; Kollman, P. A.; Case, D. A.; Singh, U. C.; Ghio, C.; Alagona, G.; Profeta, S., Jr.; Weiner, P. *J. Am. Chem. Soc.* **1984**, *106*, 765.
(40) Buckingham, A. D.; Fowler P. W. J. *J. Chem. Phys.* **1983**, *79*, 6426.
(41) Buckingham, A. D.; Fowler P. W. J. *Can. J. Chem.* **1985**, *63*, 2018.
(42) Berendsen, H. J. C.; Postma, J. P. M.; van Gunsteren, W. F.; Hermans, J. In *Intermolecular Forces*; Pullman, B., Ed.; Reidel: Dordrecht, The Netherlands, 1981; p 331.
(43) TINKER 3.8 − Software Tools for Molecular Design, Jay Ponder Lab, Department of Biochemistry & Molecular Biophysics, Washington University School of Medicine, St. Louis, MO 63110.
(44) Ryckaert, J. P.; Ciccotti, G.; Berendsen, H. J. C. *J. Comput. Phys. Soc.* **1977**, *23*, 327.
(45) Eisenberg, D.; Kauzmann, W. *The Structure and Properties of Water*; Oxford University Press: London, 1969.
(46) Hura, G.; Sorenson, J. M.; Glaeser, R. M.; Head-Gordon, T. *J. Chem. Phys.* **2000**, *113*, 9140.
(47) Berendsen, H. J. C.; Postma, J. P. M.; van Gunsteren, W. F.; DiNola, A.; Haak, J. R. *J. Chem. Phys.* **1984**, *81*, 3684.
(48) Sorenson, J. M.; Hura, G.; Glaeser, R. M., Head-Gordon, T. *J. Chem. Phys.* **2001**, *113*, 9149.
(49) Hertz, H. G. In *Water. A comprehensive treatise*; Vol. 3, Franks, F., Ed.; Plenum: New York, 1973; p 301.
(50) Franks, E. *Water A matrix of life*; Royal Society of Chemistry and Plenum: Cambridge and New York, 2000 and 1973; p 301.
(51) Tu, Y.; Laaksonen, A. *Chem. Phys. Lett.* **2001**, *329*, 283.